Conceptual Design of Rapid Circular Particle Accelerator Using High-Gradient Resonant Cavities with Fixed Frequency

Eiji Nakamura[1-6,*], Tomohiko Asai[3], Jun'ichi Sekiguchi[3], Izumi Sakai[1,2], Shin Yabukami[5,6], Yuta Sasaki[5], Yusuke Sawaki[5], Tatsuya Date[5], Jun Kudo[5], Tomofumi Ichinomiya[5], Sho Nakamura[5], Toshiki Takahashi[5], Yusuke Bannai[5], Yoshihiro Ishi[7], Tomonori Uesugi[7], Masakazu Takayama[8], Takeshi Tomomura[8], Yuma Daikoku[8], Shou Hashimoto[8], Haruhisa Koguchi[9], Shigeru Inagaki[10], Koichi kindo[11], Tsukasa Nakamura[12] and Yuko Nakamura[3]

[1]*High Energy Accelerator Research Organization (KEK), 1-1 Oho, Tsukuba, Ibaraki 305-0801 Japan*

[2]*The Graduate University for Advanced Studies (SOKENDAI), Shonan, Hayama, Kanagawa 240-0193 Japan*

[3]*Nihon University, 1-8-14 Kanda-Surugadai, Chiyoda, Tokyo 101-8308 Japan*

[4]*Fukui University, 3-9-1 Bunkyo, Fukui, Fukui 910-8507 Japan*

[5]*Tohoku Gakuin University, Faculty of Engineering, 1-13-1 Chuo, Tagajo, Miyagi 985-8537 Japan*

[6]*Tohoku Gakuin University, Research Institute for Engineering and technology, 1-13-1 Chuo, Tagajo, Miyagi 985-8537 Japan*

[7]*Kyoto University Research Reactor Institute (KURRI), 2 Asashiro-Nishi, Kumatori, Sennan, Osaka 590-0494 Japan*

[8]*Akita Prefectural University, 84-4 Ebinokuchi, Tsuchiya, Yurihonjo, Akita 015-0055 Japan*

[9]*Advanced Industrial Science and Technology (AIST), 1-1-1 Umezono, Tsukuba, Ibaraki 305-8568 Japan*

[10]*Kyushu University Research Institute for Applied Mechanics (RIAM), 6-1 Kasuga-koen, Kasuga, Fukuoka 816-8580 Japan*

[11]*The University of Tokyo, The Institute for Solid State Physics (ISSP), 5-1-5 Kashiwanoha, Kashiwa, Chiba 277-8581 Japan*

[12]*Pulse Electric Engineering Special Device Industry Co. Ltd., 311, 5-4-19 Kashiwanoha, Kashiwa, Chiba 277-0882 Japan*

Abstract: A new high-energy particle accelerator with static combined type of magnetic field and high-gradient resonant cavities is introduced for muon acceleration up to 300 MeV and proton acceleration up to 400 MeV. The accelerator concept is expected to realize Mpps-class rapid cycling high-energy particle acceleration in circular particle accelerators. Conceptual designs of the circular accelerator are discussed with an emphasis on short lifetime particles. The fundamental concept of particle acceleration and the related practical issues, which should be discussed when designing the accelerators, are described as well.

Keywords: Accelerator, Circular, Hadron, Muon, FFAG, Microtron.

INTRODUCTION

The possibility of the production and acceleration of muons by circular particle accelerators has been discussed in fundamental studies on high-energy muons and applications of GeV-class hadron particles to new energy production by using nuclear fusion reactors [1, 2]. Engineering techniques for generation of high-energy particles have been rapidly evolving, and are also used for NBI (Neutral Beam Injection) in plasma science research and exploration into a new study of muon-catalyzed fusion. Low-level electronic devices such as high-repetition rate control systems and supercomputers [3, 4], which are used for operating the particle accelerators as well as for extensive data analysis, have been substantially improved during the last decade, promoting the discussion of various types of particle accelerators. On the other hand, the electric power to beam power conversion ratio in conventional particle accelerators is very low from the viewpoint of energy production. Linear accelerators (LINACs) have better electric power conversion characteristics and can be applied to the resonant cavities with high-gradient electric fields of

*Address correspondence to this author at the High Energy Accelerator Research Organization (KEK), 1-1 Oho, Tsukuba, Ibaraki 305-0801, Japan; Tel: +81 29 864 5293; Fax: +81 29 864 3182; E-mail: eiji.nakamura@kek.jp

E-ISSN: 2408-977X/15

35 MV/m [5]. High beam intensity is achieved with long LINACs; for example, a beam of 400 MeV protons is accelerated by a 340-m long LINAC in J-PARC [6]. Such a length is not required for low intensity particle acceleration, but the overall spatial scale of LINAC is still significant. A spiral layout of LINACs is most compact, but it is desirable to reduce the number of radio frequency (RF) systems for reducing the construction cost. Cyclotrons are the most popular accelerators and are used for acceleration of various particles, but a large amount of magnetic material (ten thousand tons) is required for producing GeV-class particles. Synchrotrons are compact and are capable of producing highly energetic particles, but the output beam power is low and it is subtle unstable for pattern or AC magnetic field operation to supply high-energy beams. Moreover synchrotron cannot accelerate muons during the short lifetime, especially, because the acceleration voltage of the RF-systems is low for the synchronous condition to the time variation of bending magnets. Fixed-field alternating gradient (FFAG) accelerators [7-13] are attractive for this study because they are compact (requiring relatively small amount of magnetic material) and are capable of supplying stable beams owing to DC magnetic field operation, although the electric field of the accelerating RF devices is weak (up to 100 kV/m) because the aperture has to be large and the temporal variation of frequency has to be adjusted to the non-linear velocity of particles. We have studied an improvement of FFAG accelerator characteristic obtained by applying magnetic field configuration to main bending magnets, in order to satisfy the isochronous condition for applying high field gradient RF cavities and phase stability.

The lifetime of muons is relatively short (2.2 μs), requiring high-gradient electric fields for muon acceleration. For example, field gradients above 0.5 MV/m for classical energy treatment or above 0.28 MV/m for relativistic treatment are required for obtaining 300 MeV muons (Figure **1**), as is planned for the g-2 experiment [14]. There are no acceleration devices on conventional circular accelerators that allow producing such high gradient fields in a wide aperture, because wide range frequency modulation is required. The RF system can produce field gradients of several hundred kilo-volts per meter, but many magnets for beam handling occupy space in circular accelerators, yielding the effective net field gradient in conventional circular accelerators below 100 kV/m. There is a possibility of generating the high field gradient in an RF system operated at fixed frequency with resonant amplification in a cyclotron by applying magnetic flux density, which increases with radial position such as:

$$\upsilon = r\omega \tag{1}$$

$$\omega = \frac{qB}{m_0\gamma} \tag{2}$$

$$\gamma = \frac{1}{\sqrt{1-(\frac{\upsilon}{c})^2}} = \frac{1}{\sqrt{1-(\frac{r\omega}{c})^2}} \tag{3}$$

$$B(r) = \frac{m_0\gamma\omega}{q} = \frac{m_0\omega}{q}\frac{1}{\sqrt{1-(\frac{\omega}{c})^2 r^2}} \tag{4}$$

here r, m_0, γ, ω, q, c, υ and B indicate the radial position, the invariant mass of the particle, the Lorentz factor of the particle, the radial frequency of the RF system, the particle charge, the velocity of light in vacuum, the velocity of particles and the magnetic flux density, respectively. However an incremental dependence of the magnetic flux density on the radial direction induces vertical defocusing and crucial beam loss [15]. The sector focus cyclotron solves the beam defocusing problem, but it remains difficult to apply high gradient field RF field due to the requirements of wide aperture covering.

Circular accelerators known as microtron [16], which can be used with the high gradient field RF systems. Conventional microtrons are designed based on the notion of uniform magnetic field; thus the isochronous condition is not satisfied and acceleration times are limited to several values. On the other hand, the isochronous condition can be satisfied by using main magnets with varying magnetic fields. In microtron, space is available for installing quadruple magnets as auxiliary magnets for beam focusing. Moreover, it is possible to fabricate complicated pole surfaces for producing such magnetic field variation by using recent engineering development of machining accuracy. The possibility of particle acceleration by using a microtron with magnetic field variation is presented in this paper, summarizing the discussions at the previous meetings and conferences [17]. This novel concept bears to deliver high-energy particles at high repetition rate, especially for short lifetime particles, and will be proposed as one of the upgrade plan of the KUFFAG [18].

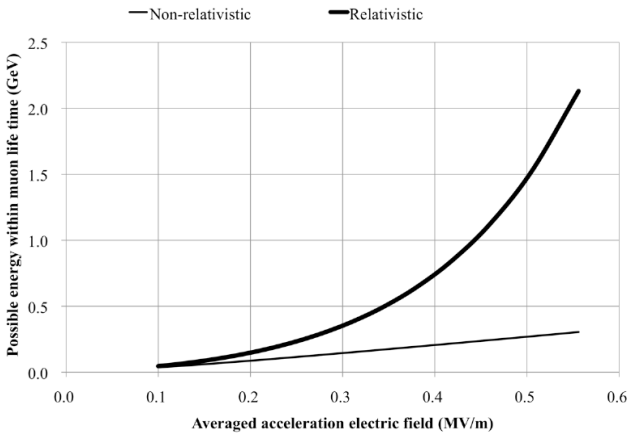

Figure1: Muon energy (during its lifetime) versus averaged accelerating electric field. The thin and the solids indicate calculation results for non-relativistic and relativistic estimations, respectively. Electric field intensity of 0.28 MV/m is required for accelerating muons to the energy of 300 MeV.

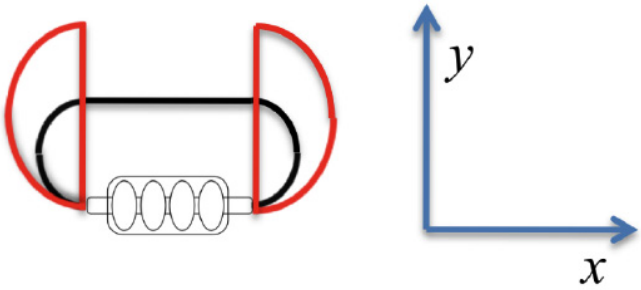

Figure 2: Coordinates system for accelerator design described in this paper.

2. ISOCHRONOUS CONDITION

In what follows, we discuss the variation vertical magnetic flux density $B(x)$ in x-direction for satisfying the isochronous condition (Figure **2**). For simplicity, we ignore the acceleration term in the kinetic equation. The equations describing the particle motion in the middle of x-y plane are:

$$m_0\gamma\frac{d\vec{\upsilon}}{dt} = q(\vec{\upsilon}\times\vec{B}) \tag{5}$$

$$m_0\gamma\frac{d\upsilon_x}{dt} = q\upsilon_y B(x) \tag{6}$$

$$m_0\gamma\frac{d\upsilon_y}{dt} = -q\upsilon_x B(x) \tag{7}$$

Assuming the initial velocity υ_0 to be positive in x-direction, $\upsilon_x = \upsilon_0 > 0$, the velocity sign in y-direction becomes negative according to Eq. 7. The horizontal motion in x-direction can be derived by integrating the product of Eq. 6 and υ_x:

$$m_0\gamma\frac{d\upsilon_x}{dt} = -q\sqrt{\upsilon_0^{\,2}-\upsilon_x^{\,2}}B(x)$$

$$m_0\gamma\frac{\upsilon_x}{\sqrt{\upsilon_0^{\,2}-\upsilon_x^{\,2}}}\frac{d\upsilon_x}{dt} = -qB(x)\upsilon_x$$

$$-\frac{m_0\gamma}{q}\sqrt{\upsilon_0^{\,2}-\upsilon_x^{\,2}} = \int_0^x B(x)dx \tag{8}$$

This equation indicates that the motion (left hand side) can be described by magnetic field variation (right hand side), and it includes a specific degree of freedom of magnetic flux density owing to the integral expression. Closed form solution of this equation cannot be obtained by using analytic methods; thus, in this paper, the variation of the magnetic flux density, which satisfies the isochronous condition, is obtained by resorting to the sequential analysis (Figure **3**). Here, the motion and the circulation time for the initial kinetic energy are obtained by solving the kinetic equation assuming uniform magnetic flux density here. To obtain the next kinetic energy in a specific region, the magnetic flux density is first obtained by employing the isochronous condition after calculating the kinetic motion in the immediately preceding region. The value of the initial magnetic flux density can be obtained by assuming smooth continuity of the magnetic flux density in Eq. 8 for the isochronous condition:

$$T_0 = \frac{L_{DS}}{\upsilon_0}+\frac{2\pi m_0}{qB_0}\gamma_0 \cong \frac{L_{DS}}{\upsilon_0+\delta\upsilon}+\frac{2\pi m_0}{qB_0}(\gamma_0+\delta\gamma) \tag{9}$$

$$B_0 \cong \frac{2\pi m_0}{qL_{DS}\delta\gamma}\frac{1}{\upsilon_0}\frac{\delta\upsilon}{\upsilon_0} \sim \frac{2\pi m_0 c}{qL_{DS}}(\beta_0\gamma_0)^3 \tag{10}$$

where T_0, L_{DS}, ß, ɣ, $ß_0$, and B_0, indicate the revolution time, the length of drift space, the ratio of the particle velocity to speed of light c, the Lorentz factor, the

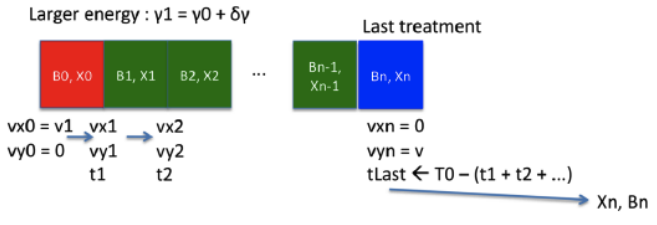

Figure 3: An outline of the sequential calculation process. For each energy level, kinetic motion is obtained by solving the kinetic equation, assuming that the magnetic flux density is uniform during all stages. The magnetic flux density during the last stage (the right cell in the figure) is calculated by applying the isochronous condition or the position condition.

velocity ratio, and the magnetic flux density for the initial energy, respectively.

Figure **4** shows the representative variation of the magnetic flux density for accelerating 40 MeV muons up to the energy of 340 MeV by using resonant cavities with the acceleration of 15 MV/unit. The particle trajectories and the overview of the accelerator are shown in Figure **5**, compared with the conventional and spiral LINAC layouts. The actual LINACs are several times longer than that shown in Figure **5**, owing to the difficulty in frequency adjustment for low-energy particles. In Figure **5**, the transit time in an RF cavity is calculated for each value of kinetic energy. The accelerator with magnetic field gradient and one resonant cavity for a ring and two cavities for pre-acceleration are possible, but the accelerator size is still large and one hundred tons of magnetic material are required, although the number of RF systems is reduced. More compact accelerators are possible to realize by using a racetrack FFAG like a double-sided microtron with magnetic field gradient and two resonant cavities. Figure **6** shows the calculated magnetic field variation. The revolution time was calculated as 105 ns. Convenient size accelerators are possible (Figure **7**).

3. TRANSVERSE MOTION

As shown in Fig**ure**s 4 and 6 in the previous section, the horizontal focusing is strong in the direction of magnetic field gradient, but the field acts to defocus the beam in the vertical direction. The fringing magnetic field at the inlet and outlet of the main magnets serves as the focusing field, and auxiliary quadruple magnets can be installed. It is difficult to describe a transverse motion with conventional Twiss-parameters for lattice designs of circular accelerators because the racetrack

Figure 4: Variation of magnetic flux density, satisfying the isochronous condition (solid line) in the case of simple microtron as a recirculating LINAC. The thin line indicates the kinetic energy *K*.

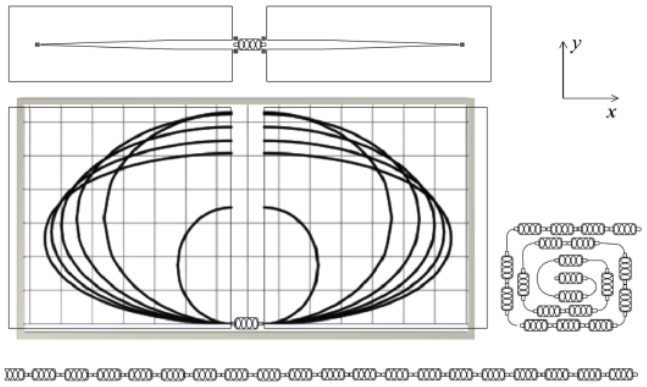

Figure 5: Representative muon trajectories for the recirculating LINAC, compared with simple LINAC (bottom panel) and spiral LINAC (right panel) sizes. Top panel shows the cross-section of main magnets. The scale unit of grids is [m].

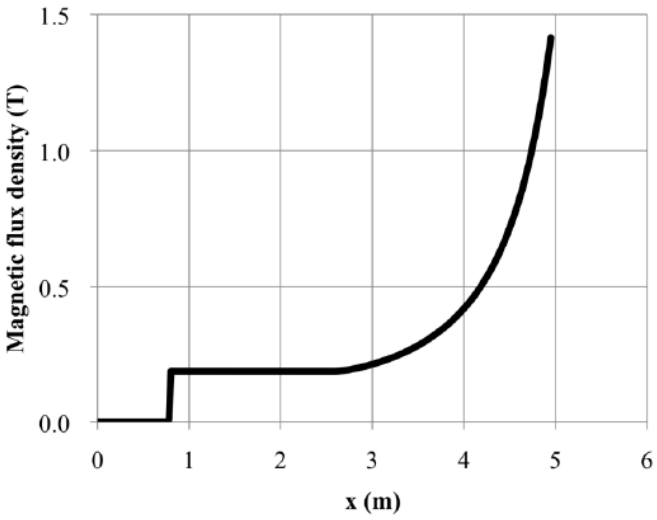

Figure 6: Variation of magnetic flux density, satisfying the isochronous condition (solid line) in the case of the recirculating LINAC.

FFAG is line symmetry although the conventional circular accelerators are point symmetry. It is, however, necessary to investigate the defocusing effect during one passage through the magnet. Denoting the vertical magnetic field gradient index by *k*, the vertical magnetic flux density B_z is given by:

$$B_z(x) \sim B_0(1+kx) \tag{11}$$

The horizontal magnetic flux density B_x can be estimated by using the Ampere-Maxwell equation, and is given by:

$$B_x(x) \sim B_0 kz \tag{12}$$

Denoting the direction of the ideal particles by *s*, the

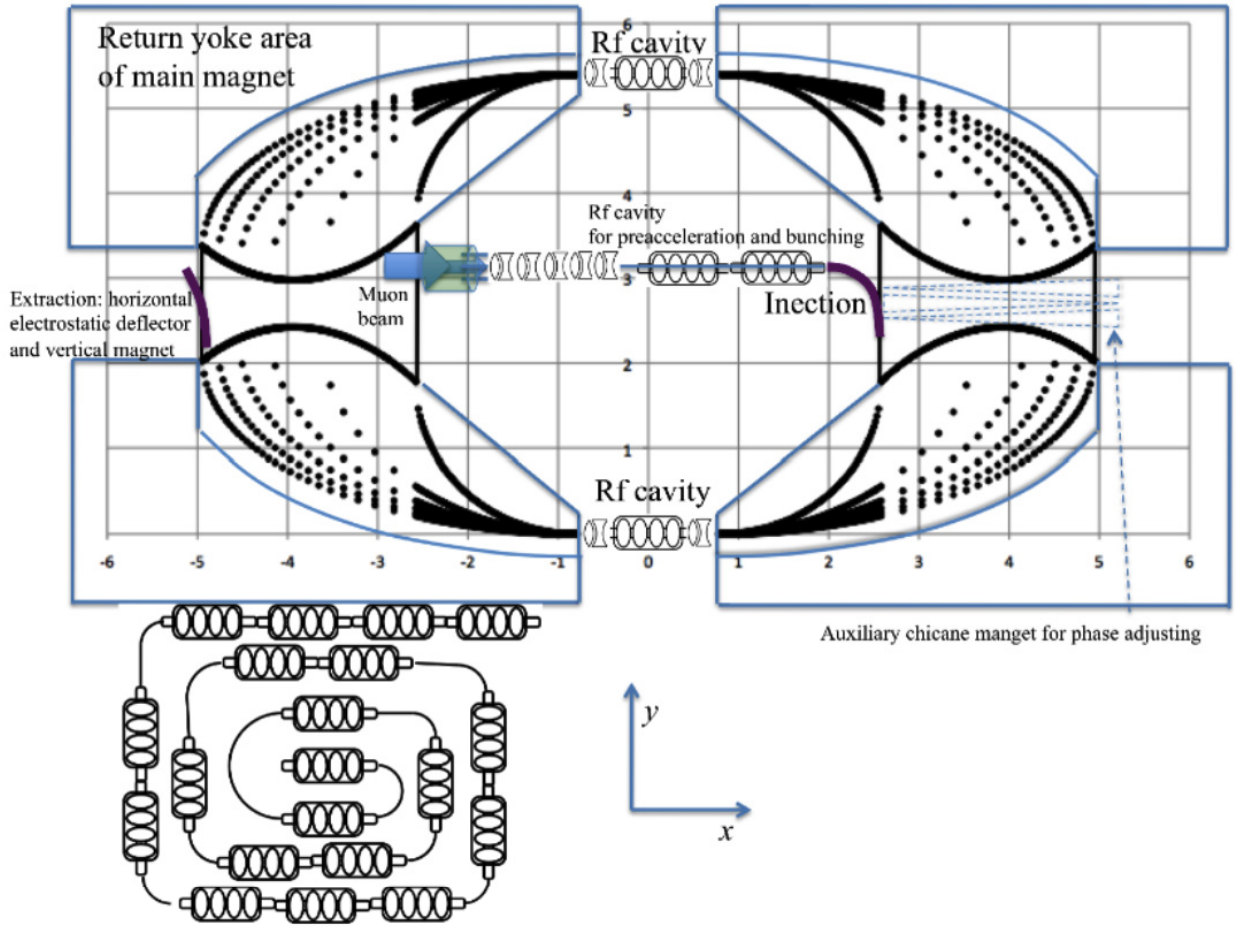

Figure 7: Representative muon trajectories for the racetrack FFAG, compared with spiral LINAC size. The scale unit of grids is [m].

vertical motion is given by:

$$m_0\gamma\frac{d^2z}{dt^2} = -q\upsilon_y B_x \sim -q\upsilon_y B_0 kz \tag{13}$$

$$\frac{d^2z}{ds^2} + (\frac{q\upsilon_y kB_0}{m_0\gamma{\upsilon_0}^2})z \sim 0 \tag{14}$$

Here, the sign of $-q\upsilon_y B_0$ is positive owing to the horizontal motion; thus the vertical divergence index K_z [m^{-1}] is estimated as following:

$$K_z = \frac{1}{\upsilon_0}\sqrt{-\frac{qB_0k\upsilon_y}{m_0\gamma}} \tag{15}$$

The value of the diverse index ranges from 0 to 1.2 m^{-1} (Figure **8**). It is possible to adopt a negative gradient magnetic field for initial energy to solve this problem because of the freedom in Eq. 8, as discussed in what follows. The field modulation in main magnets similar to those of the FFAG accelerator is one of the solutions for creating a vertical focusing as in Eq. 16 (Figure **9**). The sign of the parameter K_z^2 changes according to x, and it yields strong focusing, as shown in Eq. 18. The parameters b/B_0 = 0.1 and $1/n$ = 5 cm are sufficient for obtaining practical focusing devices. The optimal configuration for a practical accelerator can be obtained by using the same method as the conventional lattice design for the FFAG accelerators or the combined type of accelerator magnets for the rapid cycling synchrotron [19].

$$B_z(x) = B_0(1+kx) + b\sin nx \tag{16}$$

$$B_x(z) \cong (kB_0 + bn\cos nx)z \tag{17}$$

$$K_z^{\,2} = -\frac{q\upsilon_y}{m_0\gamma{\upsilon_0}^2}(kB_0 + bn\cos nx) \tag{18}$$

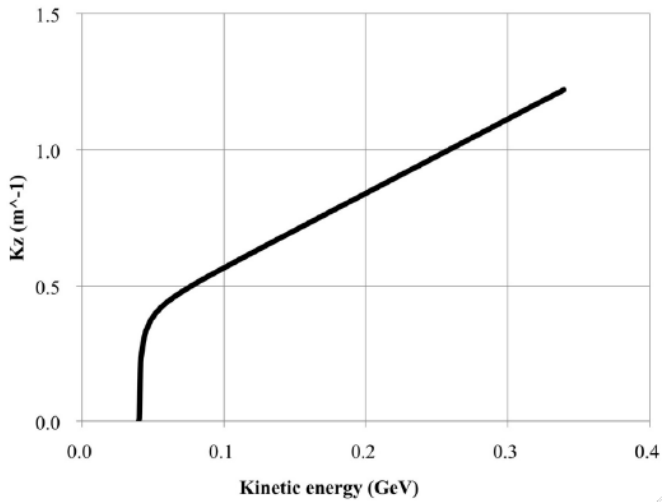

Figure 8: he maximal value of the vertical diverse constant versus kinetic energy for magnetic field configuration in Figure **4**.

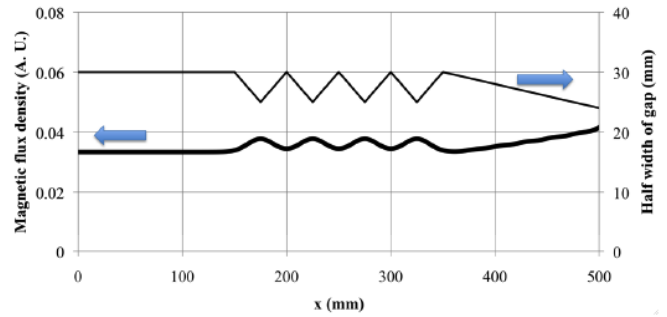

Figure 9: Magnetic field modulation. The sawtooth pole surface, marked by the thin line, can yield field modulation, as the solid line indicates.

4. LONGITUDINAL MOTION

Because the accelerated particles circulate extensively throughout the accelerator, it is very important to discuss various beam instabilities associated with such circulation. In the case of the circular accelerators with large field-gradient cavities, the particles are accelerated to the final energy within a finite number of circulations (e. g. ten circulations); thus, the instability is expected not to grow so much. On the other hand, the impact of the initial particles phase on the final energy remains an important issue. The betatron oscillation as transverse motion in beam focusing systems also contributes a temporal delay which translates into unfavorable phase differences. Phase adjustment in a circular accelerator with a 100-m circumference scale for low-mass particles acceleration has been successfully obtained for one revolution [20]. The frequency of RF systems is one of the important issues for acceleration of high-mass particles such as muons or protons, and in this case the transverse motion of the particles cannot be ignored by assuming the same phase, especially in the high-frequency regime. At lower frequencies, the cavities become large to form a resonant structure. Formation of flatness during the acceleration by electric field is one of the key issues for superimposing auxiliary higher harmonic RF to create some phase the flatness (Figure **10**). The magnetic field in the main magnets modulated by the step pole surface is shown to have a similar effect to that of the synchrotron oscillation (Figure **11**).

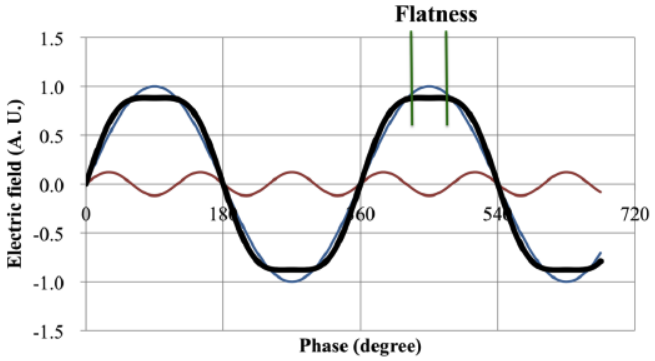

Figure 10: RF field flatness formation by superimposing with the 3rd harmonic RF with 12% of main RF field.

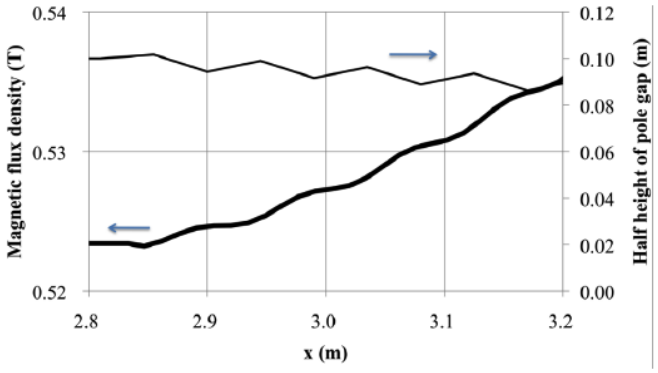

Figure 11: Magnetic field modulation (solid line) by step pole surface (thin line) in the main magnets for simulated synchrotron oscillation.

When strict temporal structure of muon beams is not required, as in some industrial applications [21-24], the muon beam can be delivered by using static electric septa [25] with thin wires of 0.1 mm radius. The turn separation in the case of the racetrack FFAG shown in Figure **7** is 0.4 MeV/0.1 mm. the free-space muon survival ratio is:

$$\frac{n(T)}{n_0} \cong e^{-\frac{T+T_0}{T_\mu}} \quad (19)$$

where T is the time that includes the relativistic effect, n is the number of muons at time T, n_0 is the initial number of muons, T_0 is the time from pion decay to the acceleration up to 40 MeV by pre-accelerators (taken here as 0.2 μs), and T_μ is the muon lifetime (taken here as 2.2 μs). Figure **12** shows the calculation results in longitudinal motion of the expected temporal structure of muons accelerated up to 300 MeV by 500 MHz RF cavities of 30 MV at peak, in the case of 40 MeV muons injected by a rectangular pulse lasting 1 μs, assuming that transverse motion and space charge effect were ignored for simplicity. Approximately 31.2% of the muons are accelerated up to the energy of 300 MeV, 47% are lost in the deceleration phase, and 21% are lost because their lifetime has exceeded, except for the beam loss due to dynamical motion throughout the low-energy beam transport line. The rest hit the electrostatic septa for beam injection and extraction. The energy-spread is mainly limited by the septum plates.

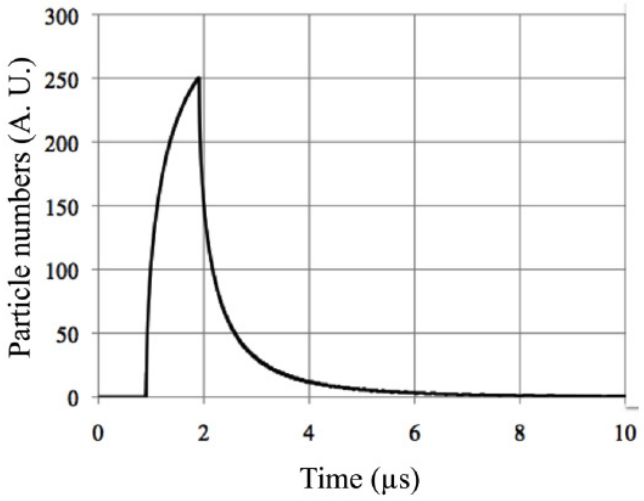

Figure 12: Temporal structure of 300 MeV muons. The vertical axis indicates the number of 300 MeV muons normalized by the initial number of muons as 1000. The survival ratio is 31.2%.

5. DISCUSSION FOR SUPPLEMENTARY DEVICES AND DEVELOPMENTS

The main components of the bending magnets and acceleration devices were described in the previous section. Additional devices are required for accelerating particles: primary transverse focusing, pre-accelerators, injection/extraction devices, and phase adjuster of chicane magnets. The typical accelerator complex including a proton storage and recycler ring [26] for pion production and cooling is shown in Figure **13**. The important issues that merit discussion and development are described in this section.

The transverse beam size at the initial energy should be sufficiently small compared with the aperture of RF orifice. The size of the muon beam is very large, and the effective number of muons in each experiment is several percent of the muons produced by using conventional techniques, because pions are produced diversely at the pion production target. The production technique of low-energy muons is one of the methods to solve the problem [27]. The MegaGauss techniques [28, 29] have been introduced recently and non-destructive solenoid magnets with strong fields of 70 T have been used in the solid-state research. The split type 30 T magnets in non-destructive solenoids can be also used as bending magnets for high-energy particle accelerators and the field variation around excitation coil is expected for beam focusing within short length at pulsed operated accelerators. The prototype of a 10 T split type magnet (Figures **14**,and **15**) is now under construction and its performance will be investigated by using the first bank power supply at Nihon University (Table **1**) [30]. Another improvement issue is the improvement of beam directivity from the pion production target. A pilot study aiming to obtain pulsed magnetic flux density above 10 T for creating the directional pion beams has been promoted to solve three specific problems: 1) the heating of excitation coils due to the Joule loss, 2) the mechanical

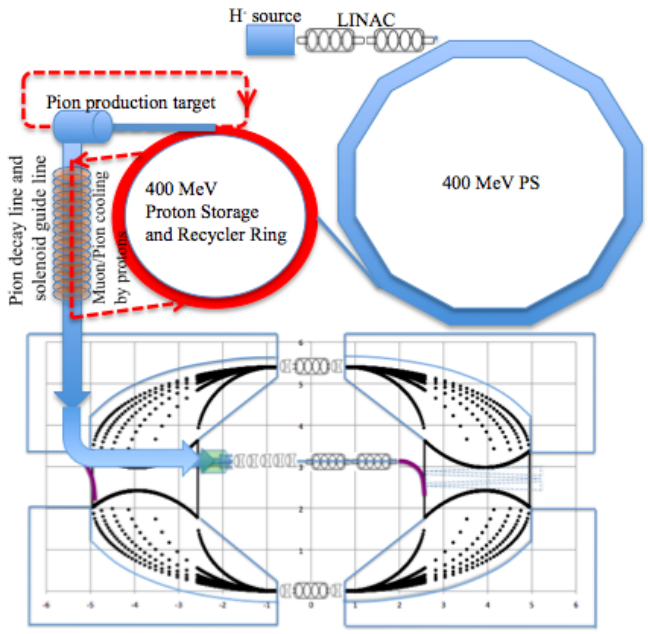

Figure 13: Overview of the entire accelerator complex for muons. In the case of the multi-purpose proton driver such as cyclotron or synchrotron, the proton storage ring or recycler ring is required to wait low-repetition rate pulse systems for high-field devices ready. The scale unit of grids is [m].

breakdown induced by the pulsed operation, and 3) the eddy current problem [31]. Heavy metals and high-density materials are used as the conventional pion targets because the cross-section for collision of primary beam particles (such as protons or deuterons) with target materials should be increased for production of high-intensity pions [32]. We prefer high-quality muon beams to high-intensity even at low-repetition rate; thus, the characteristics of various pion target materials are discussed below.

Figure **16** shows the magnetic field calculation results obtained in three scenarios of electrical conductivity. In high conductivity scenario, the magnetic flux density is reduced by the eddy current, which is induced by the pulsed excitation. Materials with high electrical resistivity, such as SiC, are preferred when pulsed excitation is considered. Magnetic materials with high electrical resistivity appear to yield the best results; however, magnetostriction and related material properties induce mechanical breakdown. A short-pulsed method using non-linear characteristics of magnetic or dielectric materials has been developed to address these issues [33-39] and related research studies are being conducted on proton storage ring [40-48] and proton driver [49-52].

Pion/muon cooling by proton beams similar to electron cooling [53] is another attractive method for modulating the pion/muon beam size, although the capture or recombination problem of pion/muon by protons should be discussed carefully. The ion/plasma channel guide technique is also useful [54, 55]. The induction acceleration located upstream of pre-accelerators [56] is expected for a wide kinetic energy profile just after pion decay.

Table 1: Representative parameters of the power supply for excitation of 10 T-manget

Parameters	Values
Charging Voltage	40 kV
Capacitance of Bank	3.75 μF
Pulse feeders	12 coaxial cables of Z_0 = 25 Ω

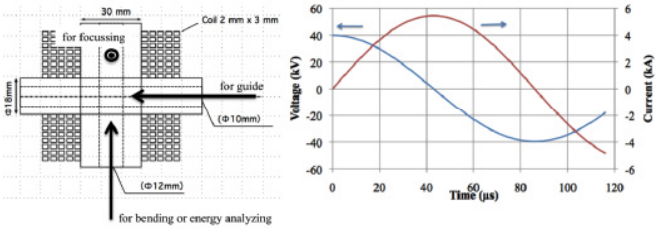

Figure 14: Overview of split type magnet (left) and the simulated excitation waveforms (right) by the first bank power supply at Nihon University. The current of 5.8 kA is expected to excite the magnet. The whole magnet will be immersed in liquid helium for cooling.

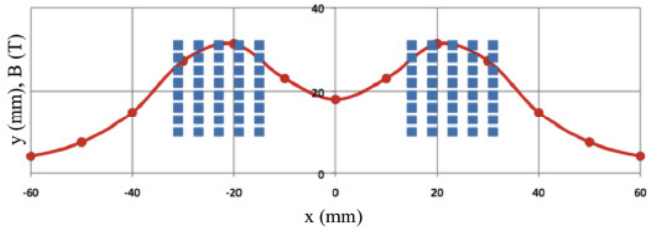

Figure 15: Variation of magnetic flux density for the split type magnet in Figure **13**, assuming the excitation urrent of 10 kA. The magnetic flux density of 10 T at the center is expected at the excitation current of 5.8 kA.

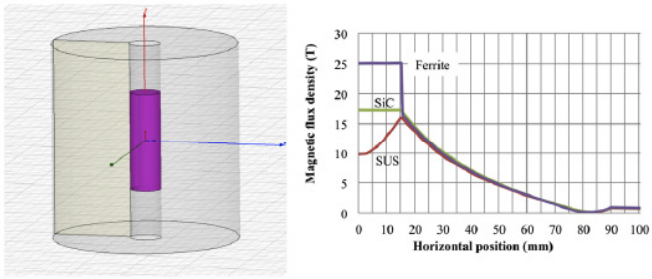

Figure 16: Pion production target estimation for in which 1-ms pulsed high magnetic field is excited for particle guiding. The center cylinder with a 30-mm radius indicates the production target, and the outer large cylinder indicates the excitation coil assembly, shown in the left panel. The right panel shows the radial profiles of the magnetic flux density for three types of target materials electrical resistivity: 100 kΩm for ferrite with saturation field of 0.3 T, 1 GΩm for silicon carbide and 1 μΩm for SUS304. The magnetic flux density is reduced near the horizontal position of zero owing to the eddy current.

Injection into the racetrack FFAG is possible by using an electrostatic inflector. Extraction is also possible by using an electrostatic deflector because the turn separation is better than that of a cyclotron due to several 100-fold higher gradient field cavities, but an additional bending system is necessary due to the weak kick angle for high-energy beam. A high-repetition kicker magnet system is applicable for fast beam ejection up to 1 kpps operation [57] by using semiconductor materials as a main switch [58-60]. It should be developed for higher repetition beam delivery. Semiconductor devices are undergoing rapid development at present, making a high-voltage and large-current switching easier to achieve; thus, higher

repetition rate kicker systems can be expected now [61]. On the other hand, a high-repetition rate operation of charging devices is a serious problem. Almost all current is dumped at dummy loads after excitation in almost all kicker systems used in high-energy particle accelerators. The recharging circuit is now under development for higher repetition rate kicker system (Figure **17**). Figure **18** shows the result for a low voltage pulse of 500 V through the coaxial cable with the characteristic impedance of 50 Ω. At present, 90% of the pulse is recharged, and 30% is recycled. The experiment was performed for 20 kV / 1.6 kA pulse, but only 15% of the pulse was recharged. A capacitor was built in the high-voltage diodes to protect against unfavorable pulses, so new high-voltage diodes have been developed now.

The kicker magnet must be of non-ferric type to prevent the unfavorable coupling with a beam and heating problem of magnet materials during high-repetition excitation. Figure **19** shows a coil configuration for to flattop formation in transverse direction for suppression of ejected beam emittance.

The feasibility of acceleration in a practical accelerator operation is especially important for multi-purpose beam delivery, and this issue is under investigation at present. Minor magnetic field deviations can be corrected by using auxiliary magnets including phase adjustment by chicane magnets. Acceleration of high-intensity beams or up to higher energy will be studied in the nearest future.

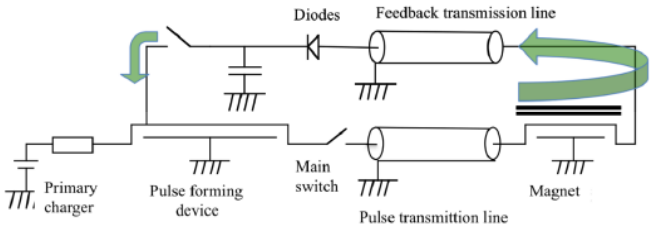

Figure 17: Prototype circuit of pulse recharging system.

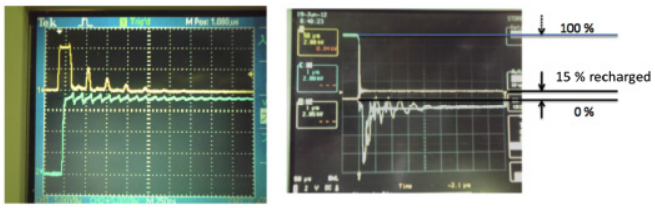

Figure 18: Experimental results for pulse recharging: low-voltage scenario (left) and high-voltage scenario (right). Horizontal axis is 2 μs/div for the left panel, and 10 μs/div for the right panel. 90% of the forward pulse of 500 V shown in the top waveform in the left panel is recharged as shown in the bottom waveform in the left panel.

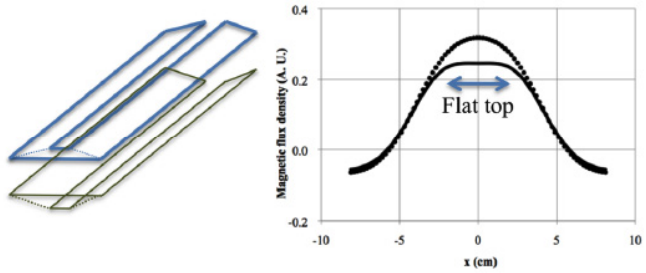

Figure 19: Overview of the kicker magnet excited by a four-turn coil (left). Horizontal uniformity is obtained by using the coil-winding method (the solid line in the right panel). Curved lines (dotted lines) are obtained in almost all cases describing the variation of the magnetic flux density excited by the simple flat four-turn coil.

6. APPLICATION TO HADRON ACCELERATION

The racetrack FFAG can be used to accelerate hadron particles. Figure **20** shows an example of the field variation for the acceleration of 40 MeV protons up to the energy of 400 MeV. The representative trajectories of protons accelerated by using the racetrack FFAG are shown in Figure **21**. The magnetic field gradient is given in the calculation where protons with the initial energy pass through. The revolution time is 258 ns. The improvement and optimization are now being studied.

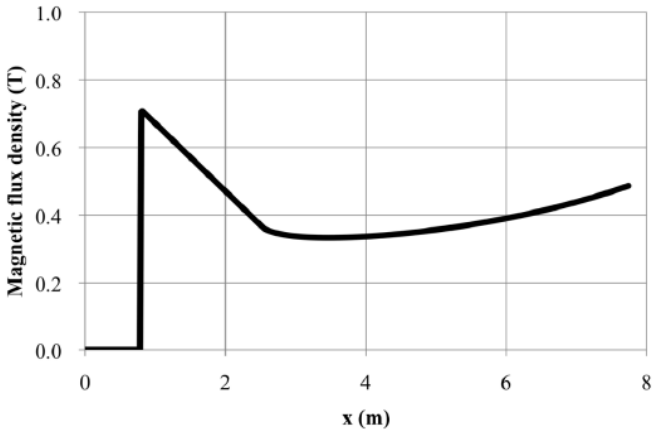

Figure 20: Variation of magnetic flux density, satisfying the isochronous condition for 40 MeV protons accelerated up to the energy of 400 MeV.

7. SUMMARY

We described a first conceptual design of the racetrack FFAG accelerator for short lifetime particles such as muons by using simulations in which field variation was applied to the microtron accelerator in

one dimension. The follow-up study on a three-dimensional optimization of magnetic field is expected to improve the accelerator performance. The acceleration method is also useful for hadron particles, and is expected to be used in the various upgrades of particle accelerators.

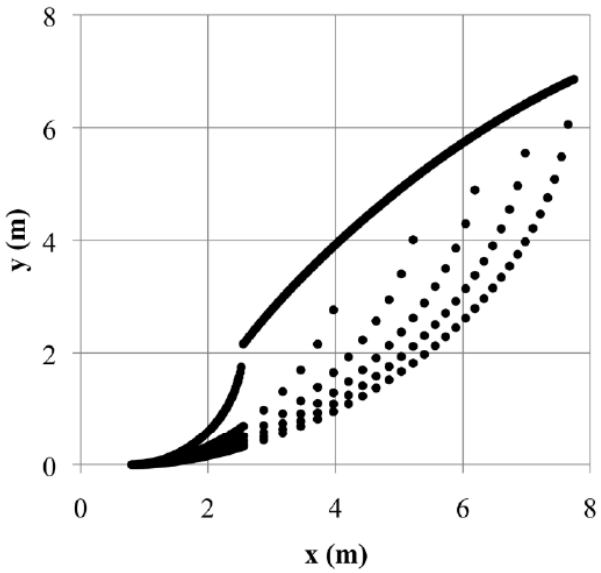

Figure 21: Example of proton trajectories of the racetrack FFAG for protons.

ACKNOWLEDGMENTS

We are grateful to Dr. Yoshiharu Mori of Kyoto University for giving an opportunity to join his project on the FFAG. We would like to express our thanks to the staff members of KEK-PS for their support and advice, and Dr. Katsuhiko Ishida and Dr. Teiichiro Matsuzaki of RIKEN, Dr. Naohito Saito and Dr. Katsunobu Oide of KEK for giving an opportunity to discuss on muon science. We give special thanks to Eng. Dai Arakawa of KEK Accelerator Laboratory, Dr. Katsumi Mochizuki of Ishinomaki Senshu University, the late Dr. Junichi Kishiro and the late Eng. Chuji Ishida for their important advice, which are formed the basis of this study. This work was supported by KAKENHI 21540310, KAKENHI 25286089, KAKENHI 26610074 and the investigative technical committee #14-01 in the Japan Society of Plasma Science and Nuclear Fusion Research (JSPF).

REFERENCES

[1] Nakamura E, Future compact fusion reactors using advanced techniques promoted rapidly in this decade, 10th academic meeting combined with nuclear fusion and energy production, 19-134, International congress center, Tsukuba, Japan, June 19th, 2014.

[2] Nakamura E, *et al*., Future compact fusion reactors using advanced techniques promoted rapidly in this decade, Investigative technical committee No. 14-01 in the Japan Society of Plasma Science and Nuclear Fusion Research (JSPF), 2014. http://research.kek.jp/people/eijinaka/h26tcjspf1401/index.html (as of Oct. 14th, 2014).

[3] Michizono S, *et al*., Digital RF Control System for 400-MeV Proton Linac of JAERI/KEK Joint Project, in: Proceedings of Linear Accelerator Conference 2002, 2002.

[4] Ebihara K, *et al*., Computer control of the system for the KEK PS, KEK-ACCELERATOR-79-4, December, 1979 (in Japanese).

[5] The International Linear Collider Technical Design Report Vol.1 - Executive Summary; Vol.2 - Physics; Vol.3 - Accelerator-Part I: R&D in the Technical Design Phase; Vol.3 - Accelerator-Part II: Baseline Design; Vol.4 - Detectors; From Design to Reality, KEK Report 2013-1: ISBN 978-3-935702-79-9.

[6] Fang Z, *et al*., Nucl. Instr. and Meth. A 767 (2014) 135. http://dx.doi.org/10.1016/j.nima.2014.08.014

[7] Ohkawa T. Bull. Phys. Soc. Jpn. (1953).

[8] Mori Y. Nucl. Instr. and Meth. A 451 (2000) 300. http://dx.doi.org/10.1016/S0168-9002(00)00555-6

[9] Machida S. Nucl. Instr. and Meth. A 503 (2003) 41. http://dx.doi.org/10.1016/S0168-9002(03)00639-9

[10] Machida S. Nucl. Instr. and Meth. A 503 (2003) 322. http://dx.doi.org/10.1016/S0168-9002(03)00707-1

[11] Keil E, Sessler AM. Nucl. Instr. and Meth. A 538 (2005) 159. http://dx.doi.org/10.1016/j.nima.2004.08.139

[12] Antoine S, *et al*., Nucl. Instr. and Meth. A 602 (2009) 293. http://dx.doi.org/10.1016/j.nima.2009.01.025

[13] Yonemura Y, *et al*., Nucl. Instr. and Meth. A 576 (2007) 294. http://dx.doi.org/10.1016/j.nima.2006.11.072

[14] Saito N. A novel precision measurement of muon g - 2 and EDM at J-PARC, GUT2012, in: AIP Conference Proceedings, Vol. 1467 (2012).

[15] Lee SY. Accelerator Physics, World Scientific, ISBN 981–02–3709-X.

[16] Kamei T, Kihara M. Accelerator Science, ISBN 4–621-03873-7 C 3342.

[17] Hikaru Sano, *et al*., Fundamental design of compact high-energy hadron accelerator for nuclear fusion driver, in: Proceedings of the 30th annual meeting of the Japan Society of Plasma Science and Nuclear Fusion Research, 05aE52P, Tokyo Institute of Technology, Ookayama, Tokyo, Japan, December 3-6, 2013.

[18] Mori Y. Nucl. Instr. and Meth. A 562 (2006) 591. http://dx.doi.org/10.1016/j.nima.2006.02.044

[19] Takikawa K, *et al*., The EKK Booster Magnet, KEK-75-3, Jun. 1975, pp. 48.

[20] Hwang JG, *et al*., Nucl. Instr. and Meth. A 562 (2006) 591. http://dx.doi.org/10.1016/j.nima.2006.02.044

[21] μCF proceedings eds. By Nagamiya K, Ishida K. in Hyperfine Interactios (2000).

[22] Nagamine K, *et al*., Physica B 289-290 (2000) 116. http://dx.doi.org/10.1016/S0921-4526(00)00298-2

[23] Nagamine K, *et al*., Nucl. Instr. and Meth. A 356 (1995) 585. http://dx.doi.org/10.1016/0168-9002(94)01169-9

[24] Nagamine K, *et al*., Phys. Rev. Lett. 74 (1995) 585. http://dx.doi.org/10.1103/PhysRevLett.74.4811

[25] Tomizawa M, *et al*., Instr. and Meth. A 326 (1993) 339. http://dx.doi.org/10.1016/0168-9002(93)90842-6

[26] Fermilab Recycler Ring Technical Design Report Revision 1.2 Nov. 5, 1996.

[27] Bakule P. Nucl. Instr. and Meth. A 753 (2014) 97. http://dx.doi.org/10.1016/j.nima.2014.03.045

[28] Kindo K. the production of 80 T non-destructive magnets and the application for the solid state research, Solid State Physics, 38 (2003) 15. (written in Japanese)

[29] Takeyama S, Kojima E. A copper-lined magnet coil with maximum field of 700 T for electromagnetic flux compression, J. Phys. D: Appl. Phys. 44 (2011) 425003(8pp).

[30] Sekiguchi J. (private communication).

[31] Nakamura E, *et al*., J. Magn. Soc. Jpn. 35 (2011) 96. http://dx.doi.org/10.3379/msjmag.1102R005

[32] Bungau A, *et al*., Phys. Rev. ST Accel. Beams 17, 034701 (2014). http://dx.doi.org/10.1103/PhysRevSTAB.17.034701

[33] Nakamura E, *et al*., A modification plan of the KEK 500 MeV booster to an all ion accelerators (an injector-free synchrotron), in: Proceedings of the 2007 Particle Accelerator Conference, Albuquerque, New Mexico, USA, June 21-29, 2007, p. 1492.

[34] Nakamura E. Nucl. Instr. and Meth. A 612 (2009) 50. http://dx.doi.org/10.1016/j.nima.2009.08.090

[35] Nakamura E. Nucl. Instr. and Meth. A 618 (2010) 22. http://dx.doi.org/10.1016/j.nima.2010.02.115

[36] Nakamura E, Nakamura E, Impulse Q-magnet and Combined-type Kicker Magnet for Fast eXtraction, KEK Internal Report ASN-477, 2004 (written in Japanese).

[37] Takasu Y, *et al*., Impulse Q-magnet and Combined-type Kicker Magnet for Fast eXtraction Part II, KEK Internal Report ASN-494, 2006 (written in Japanese).

[38] Nakamura E, *et al*., Jpn. J. Appl. Phys. 36 (1997) 889. http://dx.doi.org/10.1143/JJAP.36.889

[39] Nakamura E, *et al*., Nucl. Instr. and Meth. A 624 (2010) 554. http://dx.doi.org/10.1016/j.nima.2010.09.144

[40] Nakamura E, Injection/ejection devices for AIA, in: Proceedings of the Ninth Accelerator and Related Technology for Application (ARTA2007), TIT, Tokyo, Japan, June 21-22 (2007) 21p6.

[41] Sato H, *et al*., A switching power supply for the PFL kicker magnet, in: Proceedings of PAC 2003, 1165.

[42] Nakamura E, *et al*., Kicker systems for ejection from 3 GeV RCS in J-PARC, in: Proceedings of the 14th Symposium on Accelerator Science and Technology, 1P035, Tsukuba, Japan, November 2003.

[43] Tomizawa M, *et al*., New optics design of injection /fast extraction/abort lines of J-PARC main ring, in: Proceedings of PAC07, Albuquerque, New Mexico, USA, June 25-29, 2007, pp.1508. http://dx.doi.org/10.1109/pac.2007.4440805

[44] Nakamura E, *et al*., A modification plan of the KEK 500 MeV booster to an all ion accelerators (an injector-free synchrotron), in: Proceedings of the 2007 Particle Accelerator Conference, Albuquerque, New Mexico, USA, June 21-29, 2007, p. 1492.

[45] Nakamura E, *et al*., Permanent Magnets for the 500 MeV Accumulator Ring of the Intensity Doubler Project in KEK-PS, P2oth11, in: Proceedings of the High Energy Accelerators (HEACC 2001), Tsukuba, Mar. 29th, 2001.

[46] Kawakubo T, *et al*., Permanent magnet generating high and variable septum magnetic field and its deterioration by radiation, in: Proceedings of the European Particle Accelerator Conference, Lucerne, Switzerland, July 5-9, 2004, pp. 1696-1698.

[47] Nakamura E, *et al*., Permanent Magnets for the 500 MeV Accumulator Ring of the Intensity Double Project in KEK-PS, in: Proceedings of the 18th International Conference on High Energy Accelerators (HEACC2001), Tsukuba international congress center, Tsukuba, Japan, March 26-30 (2001) P2oth11. http://conference.kek.jp/heacc2001/ (as of Oct. 2nd, 2014).

[48] Brown BC, *et al*., Time dependence and temperature stability of the permanent magnets for Fermilab antiproton recycler ring, IEEE Trans. Applied Supercon., Vol. 10, No.1, (2000) 879. http://dx.doi.org/10.1109/77.828371

[49] Takayama K, *et al*., KEK-PS upgrade scenario: 500 MeV Accumulator and Superbunch acceleration, in: Proceedings of EPAC2000.

[50] Takayama K, *et al*., Intensity Doubler: a proposal for a major upgrade of the KEK 12 GeV-PS, in: HEACC2001 (2001) P2oth17.

[51] Nakamura E, *et al*., Nucl. Instr. and Meth. A 640 (2012) 29. http://dx.doi.org/10.1016/j.nima.2011.03.022

[52] Nakamura E, *et al*., Japan Patents: JP4543182, JP4697961, JP5447929, JP5448149, JP5565798, JP5590550.

[53] Edwards DA, Syphers MJ. An Introduction to the Physics of High Energy Accelerators, ISBN 0–471–55163–5.

[54] Tauschwitz A, *et al*., Experimental investigations of plasma lens focusing and plasma channel transport of heavy ion beams, in: Proceedings of the Particle Accelerator Conference 1995 Vol. 3, (1995) 1852. http://dx.doi.org/10.1109/pac.1995.505384

[55] Saito K. X-band Prebunched FEL Amplifier, doctoral dissertation of the Graduate University for Advanced Studies, Japan (1995).

[56] Kishiro J, *et al*., Nucl. Instr. and Meth. A 451 (2000) 304. http://dx.doi.org/10.1016/S0168-9002(00)00557-X

[57] Ishi Y, *et al*., Nucl. Instr. and Meth. A 472 (2001) 639. http://dx.doi.org/10.1016/S0168-9002(01)01323-7

[58] Kishiro J, *et al*., Rapidly Switched Accelerating Devices for Induction Synchrotrons, in: Proceedings of EPAC2000, 1966-1968 (2000).

[59] Sato H, *et al*., Pulsed power supply for the kicker magnet with SI-Thyristors, in: Proceedings of Recent Progress in Induction Accelerators (RPIA 2002), W4-3, KEK, Tsukuba, Japan, October 29-31, 2002.

[60] Jiang W, *et al*., Compact Solid-State Switched Pulsed Power and Its Applications, in: Proceedings of the IEEE, Vol.92, No.7, July, 2004.

[61] Watson J, *et al*., A solid-state modulator for high speed kickers, in: Proceedings of the Particle Accelerator Conference 2001, June 18-22 (2001) 253. http://dx.doi.org/10.1109/pac.2001.988237

Received on 15-04-2015 Accepted on 13-05-2015 Published on 15-06-2015

http://dx.doi.org/10.15379/2408-977X.2015.02.01.2